Natural Resources Canada | Ressources naturelles Canada

GEOLOGICAL SURVEY OF CANADA
OPEN FILE 8949

Mercury concentrations in near-surface lake sediments of the Yellowknife area, Northwest Territories, Canada

J.M. Galloway, M.J. Palmer, M.B. Parsons, N.A. Nasser, H. Falck, H.M. Roe, and R.T. Patterson

2023

Canada

ISSN 2816-7155
ISBN 978-0-660-47584-4
Catalogue No. M183-2/8949E-PDF

GEOLOGICAL SURVEY OF CANADA
OPEN FILE 8949

Mercury concentrations in near-surface lake sediments of the Yellowknife area, Northwest Territories, Canada

J.M. Galloway [1], M.J. Palmer[2], M.B. Parsons[3], N.A. Nasser[4], H. Falck[5], H.M. Roe[6], and R.T. Patterson[4]

[1]Geological Survey of Canada, 3303-33rd Street N.W., Calgary, Alberta
[2]Aurora Research Institute, Aurora College, 5004-54th Street, Yellowknife, Northwest Territories
[3]Geological Survey of Canada, 1 Challenger Drive, P.O. Box 1006, Dartmouth, Nova Scotia
[4]Department of Earth Sciences, Carleton University, 1125 Colonel By Drive, Ottawa, Ontario
[5]Government of the Northwest Territories, P.O. Box 1320, Yellowknife, Northwest Territories
[6]Department of Natural and Built Environment, Queen's University, Stranmillis Road, Belfast, United Kingdom

2023

© His Majesty the King in Right of Canada, as represented by the Minister of Natural Resources, 2023

Information contained in this publication or product may be reproduced, in part or in whole, and by any means, for personal or public non-commercial purposes, without charge or further permission, unless otherwise specified.
You are asked to:
- exercise due diligence in ensuring the accuracy of the materials reproduced;
- indicate the complete title of the materials reproduced, and the name of the author organization; and
- indicate that the reproduction is a copy of an official work that is published by Natural Resources Canada (NRCan) and that the reproduction has not been produced in affiliation with, or with the endorsement of, NRCan.

Commercial reproduction and distribution is prohibited except with written permission from NRCan. For more information, contact NRCan at copyright-droitdauteur@nrcan-rncan.gc.ca.

Permanent link: https://doi.org/10.4095/331434

This publication is available for free download through GEOSCAN (http://geoscan.nrcan.gc.ca/).

Recommended citation
Galloway, J.M., Palmer, M.J., Parsons, M.B., Nasser, N.A., Falck, H., Roe, H.M., and Patterson, R.T., 2023. Mercury concentrations in near-surface lake sediments of the Yellowknife area, Northwest Territories, Canada; Geological Survey of Canada, Open File 8949, 27 p. https://doi.org/10.4095/331434

Publications in this series have not been edited; they are released as submitted by the author.

Table of Contents

ACKNOWLEDGEMENTS 1
PROJECT SUMMARY 1
1. INTRODUCTION 1
2. STUDY AREA 3
2.1 Bedrock and surficial geology 5
3. METHODS 7
3.1 Sampling 7
3.2 Mercury analysis 14
RESULTS AND DISCUSSION 14
CONCLUSIONS 21
REFERENCES 21

ACKNOWLEDGEMENTS

This project was carried out with financial support from the Geological Survey of Canada, GEM GeoNorth Program, Environmental Geoscience Program - Metal Mining Project, Northern Baselines Activity (2014-2019), Environmental Geoscience Program - Long-term hydrological dynamics of the Mackenzie River Basin Project (2019-2024), Polar Knowledge Canada (Project# 1519-149 to JMG and RTP), Arctic Net (Project #51 to JMG), Natural Sciences and Engineering Research Council of Canada (NSERC; RGPIN 41665-2012 to RTP), the Government of the Northwest Territories via the Cumulative Impact Monitoring Program (Project #151 to MP) and the Northwest Territories Geological Survey (HF), the Tibbitt to Contwoyto Winter Road Joint Venture, Carleton University, and Queen's University, Belfast. We are grateful to Lisa Neville, Andrew Macumber, Shantal Goldsmith, Carley Crann, Fritz Griffith, Thomas Hadlari, Ava Hadlari, and the staff of the Tibbitt to Contwoyto Winter Road, particularly then Director Erik Madsen, for their in-kind contributions and assistance in sample collection. We thank Great Slave Helicopters for air support during the sampling campaign. We thank Lori Campbell for analyzing the mercury content of all samples at GSC-Atlantic. Galloway et al. (2012, 2015, 2018) report sediment particle size and inorganic and organic sediment geochemical data, including Hg measured by ICP-MS from regional lakes, including some of those reported here. Palmer et al. (2015) report surface water chemistry of regional lakes, including some of those reported here. Macumber et al. (2012) report surface water and sediment inorganic geochemistry of the suite of sample lakes from the Tibbitt to Contwoyto Winter Road. Macumber et al. (2018) report and discuss grain size data from the samples collected along the Tibbitt to Contwoyto Winter Road. Sample collection and research was carried out under Aurora Research Institute License numbers: 14435 and 15858. We thank Dr. Manuel Bringué for his internal review.

PROJECT SUMMARY

Total mercury (Hg) concentration was measured in 175 near-surface sediment samples from 169 lakes in the central Northwest Territories. The lakes are located west and southwest of the City of Yellowknife in the Western Interior Platform, near the City of Yellowknife, east and southeast of the City of Yellowknife along the Ingraham Trail (Highway 4), and northeast of the City of Yellowknife along the Tibbitt to Contwoyto Winter Road. Total Hg in the sediment samples ranges from 3 to 317 $\mu g \cdot kg^{-1}$. The sediments sampled from lakes in the Western Interior Platform had significantly lower sedimentary Hg concentrations than the other regions.

1. INTRODUCTION

Abundant gold mineralization in the Slave Geological Province of the Northwest Territories (NT), Canada, led to the establishment of numerous mines from the late 1930s to the present day, such as Giant Mine [1948-1999], Con Mine [1938-2003], and Tundra/Salmita [1964-1968 & 1983-1986], and the region remains highly prospective for additional gold development. Historical mineral processing and waste-disposal practices at some mines (Giant, Con, Discovery, and Tundra/Salmita mines) that were employed prior to the development of more efficient technologies and stringent environmental regulations resulted in substantial contamination by arsenic (As), some of which is in a form that is highly toxic, soluble, and bioaccessible (As trioxide, As_2O_3) and

persists in regional lake sediments (Galloway et al., 2018; Schuh et al., 2018; Van Den Berghe et al., 2018).

Regional contamination by As in lake sediments extends more than 30 km from the historic Giant Mine roaster stack (Galloway et al., 2018; Cheney et al., 2020; Jasiak et al., 2021) but is most pronounced within 17.5 km (Palmer et al., 2015), and is focused downwind to the NW (Palmer et al., 2015; Galloway et al., 2018). Contamination is particularly pronounced in Pocket Lake, located on the Giant Mine property, where As concentration in sediments reaches up to 30,000 $mg \cdot kg^{-1}$ (Thienpont et al., 2016) above a background of 250 $mg \cdot kg^{-1}$ at 50.25 cm depth (pre-1900 AD) (Thienpoint et al., 2016) and <150 $mg \cdot kg^{-1}$ in strata dated near 1100 cal yr BP (Patterson et al., 2017; Hutchinson et al., 2019; Hamilton et al., 2021). The concentration of As ranges into the 1000s of $mg \cdot kg^{-1}$ in near-surface sediments of nearby lakes as well (Galloway et al., 2015, 2018). A more detailed description of the history of mining and regional contamination by As is presented in Galloway et al. (2012, 2015, 2018), Jamieson (2014), Palmer et al. (2015), and Sandlos and Keeling (2016). This contamination has been the focus of several subsequent studies on the distribution of As (e.g., Jasiak et al., 2021), impact on aquatic biota (Nasser et al., 2014; Cott et al., 2016; Persaud et al., 2021; Sivarajah et al., 2022) and human health assessments (Cheung et al., 2020).

Although the predominant element of concern associated with gold projects in the region has been As, the concentrations of other elements, such as mercury (Hg) and antimony (Sb), are elevated in environmental media near many of these sites (Houben et al., 2016; Palmer et al., 2019). Mercury amalgamation was used at Giant Mine for gold recovery from 1948 until 1958 (INAC, 2007; Mackenzie Valley Review Board, 2013) and Hg was often released as a by-product of ore roasting and smelting. Few site-specific studies have been done (Thienpoint et al., 2016; Pelletier et al., 2021) and little work has been focused on Hg in the regional environment (Houben et al., 2016; Pelletier et al., 2021). Mercury released to the atmosphere can be redeposited through wet/dry deposition in nearby catchment soils and surface waters. However, due to the long (~1 to 1.5 years) atmospheric residence time of gaseous mercury [Hg(0)], Hg deposition in lakes surrounding a point source may not display a local response (Houben et al., 2016). Thienpoint et al. (2016) show that Hg levels increased by 2000% to greater than 2.0 $\mu g \cdot g^{-1}$ in the upper sediments of Pocket Lake (located on the Giant Mine property), deposited after the late 1950s. In contrast, Houben et al. (2016) in their analysis of 25 lakes within a 25 km radius of the historic Giant Mine roaster stack did not find a correlation with distance and total Hg concentration (range: 0.49 to 2.41 ng/L) in surface waters. However, methylmercury (MeHg) concentrations were higher in lakes closer to the former Giant Mine. Houben et al. (2016) suggest that the high sulfate emissions associated with historical roasting activities may have enhanced rates of Hg methylation in lakes closer to the point source of emission, as increased sulfate concentrations (up to above 50 mg/L) can stimulate sulfate reducing bacteria activity (Gilmour et al., 1992). The greater MeHg concentrations in lakes closest to the historic roaster stack may reflect an indirect response to the increase in sulfate concentration associated with bedrock geology (Yellowknife Bay Formation metavolcanics; Houben et al., 2016) and/or to sulfate emissions from Giant Mine and subsequent deposition into the nearby catchments.

Pelletier et al. (2021) studied lead (Pb) and Hg in six bogs and sediments of five lakes of the Yellowknife region. They report total Hg concentration in lake sediments deposited in pre-

industrial times as ranging between 28 ± 3 $\mu g \cdot kg^{-1}$ and 47 ± 5 $\mu g \cdot kg^{-1}$, depending on the site, with a mean for all samples of 39 $\mu g \cdot kg^{-1}$ and a range of 23 to 54 $\mu g \cdot kg^{-1}$ (n=116). Not surprisingly, the total Hg concentration in the pre-industrial lake sediments examined by Pelletier et al. (2021) was greater at sites with more organic matter content, as determined by them using loss-on-ignition. However, this relationship was not significant in their study (when using all samples from all lakes), possibly due to low sample size (n=5 sites) (as the authors note) or due to the fact that it is the character, rather than quantity, of organic matter that is most important in terms of sequestering Hg (and other elements; see Galloway et al., 2018) in lake sediments (Kainz and Lucotte, 2006; Haitzer et al., 2002; Sanei et al., 2014; Outridge et al., 2007, 2019). Two of the five lakes sampled by Pelletier et al. (2021) are located in the Taiga Plain ecozone, west of Yellowknife and overlying bedrock of the Western Interior Platform (Figs. 1, 2). Three of their study lakes, and all six bogs studied by them, are located in the Taiga Shield ecoregion that is underlain by components of the Slave Geological Province (Figs. 1, 3). Organic matter appeared to be an important control on Hg accumulation in at least two of the lakes in the Taiga Shield. At one site, lake PL2, Hg concentration increased by only 20 $\mu g \cdot kg^{-1}$ over the length of the core and remained constant after ~1998. Mercury concentration was strongly related to organic content in this lake. In lake HL1, the trend was similar, but the maximum increase of Hg was 40 $\mu g \cdot kg^{-1}$, and the relationship to organic matter weaker but still significant. In the sediments of the Taiga Shield lake closest to Yellowknife, lake IGT3-2, a distinct peak in Hg concentration occurred in sediment that accumulated between 1948 and 1981, reaching a maximum of 133 $\mu g \cdot kg^{-1}$. Following this peak, Hg concentrations declined but remained greater than in pre-industrial sediment. Total Hg concentration was not related to organic matter concentration in this lake. In the lakes located on the Taiga Plain, there was no consistent relationship between sediment organic matter and Hg concentration and Taiga Plains lakes had declining Hg concentration in their sediments after 1975 (lake CL2) and after 1997 (lake HW3-1). In summary, Taiga Plains lakes had lower total Hg concentration in their sediment, and Taiga Shield lakes had higher anthropogenic Hg flux to their sediment (fig. 8, Pelletier et al., 2021; see their paper for methods of anthropogenic Hg flux modelling). These authors conclude that Taiga Shield lakes were slower to recover from a reduction in North American atmospheric emissions of Hg and Pb because accumulation rates of Pb and Hg continued to increase despite decreasing atmospheric deposition in the region. They conclude that as anthropogenic metal accumulation in these lakes was no longer driven by atmospheric emissions, input must be from "external factors affecting catchment contributions", such as legacy pollution. Geogenic sources of Hg, and other elements involved in the sequestration of Hg (e.g., sulphur) may also be involved in areas underlain by mineralized bedrock. In the pre-industrial peat, Hg concentrations were 42 ± 15 $\mu g \cdot kg^{-1}$ (n=172, max 96 $\mu g \cdot kg^{-1}$) (Pelletier et al., 2021). Similar to some of the lake profiles, sub-surface peaks of Hg (to between ~140-250 $\mu g \cdot kg^{-1}$) also occurred in peat cores corresponding to peat that accumulated between 1950 and 1980 and these peaks were followed by a return to pre-industrial Hg concentrations in uppermost layers. This body of work indicates that additional research is needed to better understand controls on Hg mobility and fate in the study region. Spatial surveys and additional temporal studies are thus needed.

2. STUDY AREA

The Hay River Lowland of the Taiga Plains Ecozone occurs west and south of Great Slave Lake (Ecosystem Classification Group, 2007). This broad lowland plain is characterized by a subhumid

mid-boreal climate. The mean summer temperature is 13°C and mean winter temperature is -19°C. Mean annual precipitation ranges from 350 to 450 mm. Vegetation is composed of closed mixed stands of trembling aspen (*Populus tremuloides*), balsam poplar (*Populus balsamifera*), white spruce (*Picea glauca*), balsam fir (*Abies balsamea*), and black spruce (*Picea mariana*) on dry or boggy sites. Poorly drained fens and bogs cover 30% of the ecoregion and also support larch (*Larix laricina*).

The Great Slave Lake Plain of the Taiga Plains Ecozone occurs west of the North Arm of Great Slave Lake (Ecosystem Classification Group, 2007). The ecoregion has a low subarctic climate and is underlain by discontinuous permafrost. Mean annual temperature is -6°C with a mean summer temperature of 11.5°C and mean winter temperature of -25°C. Mean annual precipitation ranges between 225 to 300 mm. The ecoregion is dominated by open stands of black spruce and groundcover of Labrador tea (*Ledum decumbens*), ericaceous shrubs, and mosses. Wetlands cover about half of the region.

The Yellowknife study area occurs south of the treeline and lies within the Great Slave Lake Lowland and Great Slave Lake Upland ecoregions of the Taiga Shield Ecozone (Ecosystem Classification Group, 2007). Climate is sub-humid, high-boreal, and characterized by a mean summer temperature of 11°C and a mean winter temperature of -21.5°C. Mean precipitation ranges between 200 and 375 mm. Vegetation is composed of closed stands of trembling aspen, balsam poplar, paper birch (*Betula papyrifera*), and jack pine (*Pinus banksiana),* with white spruce and black spruce dominating later successional stands. Poorly drained fens and bogs are covered with open stands of larch and black spruce. The City of Yellowknife and surrounding area is located in the southwestern Slave Geological Province, District of Mackenzie (Fig. 1). Elevation in the region rises gradually from 157 m above sea level (MASL) near Great Slave Lake to approximately 400 MASL north of 63° latitude. The Yellowknife River is the main drainage for the area. Its southern outlet flows into Yellowknife Bay, Great Slave Lake. Many lakes east of Yellowknife lie within the Cameron River-Prelude Lake watershed. Drainage in the region is influenced by bedrock structure; numerous small elongate lakes have formed along fault and joints in the bedrock.

Northeast of Yellowknife, the Tibbitt to Contwoyto Winter Road (TCWR) traverses the central Slave Geological Province (Fig. 4). The southern end of the TCWR begins in the Tazin Lake Upland Ecoregion of the Taiga Shield Ecozone and travels north into the Coppermine River Upland Ecoregion of the Southern Arctic Ecozone near latitudinal treeline and then into the barrenlands of the Takijuq Lake Upland Region of the Southern Arctic Ecozone near Lac de Gras (Ecosystem Classification Group, 2007). The Coppermine River Upland Ecoregion is characterized by a high subarctic climate with a mean summer temperature of 9 °C and mean winter temperature of -24.5 °C. Annual precipitation ranges from 200 to 300 mm. Vegetation consists of open, stunted stands of black spruce and larch with lesser amounts of white spruce. Shrub or ground cover in these open communities consists of dwarf birch (*Betula glandulosa*), willow (*Salix* spp.), ericaceous shrubs, such as northern Labrador tea and red bearberry (*Arctostaphylos rubra*), cotton grass (*Eriophorum* spp.), and lichen. Poorly drained areas support tussocks of sedge (*Carex* spp.), cotton grass and sphagnum moss (*Sphagnum* spp.). Low shrub tundra consisting of dwarf birch and willow are also common in this ecoregion. Climate of the Takijuq Lake Upland Ecoregion of the Southern Arctic Ecozone is characterized as low arctic, with a mean summer temperature of 6°C and mean winter temperature of -26.5°C (Wiken, 1986).

Annual precipitation ranges from 200 to 300 mm. Vegetation is composed of shrub tundra consisting of dwarf birch, willow, Labrador tea, and ericaceous plants. Low-lying sites support willow, sphagnum moss, and sedge. Scattered stands of spruce may occur along the southern boundary of the ecoregion. Lakes northeast of the City of Yellowknife along the Tibbitt to Contwoyto Winter Road and associated waterbodies drain into four primary drainage basins: the Great Slave Lake and Mackenzie River Drainage Basin, the Coppermine River Drainage Basin, the Back River Drainage Basin, and the Hood and Burnside rivers Drainage Basin. On the southern end, within the Great Slave Lake and Mackenzie River Drainage Basin, the winter road traverses the Cameron, Beaulieu, and Lockhart river watersheds.

2.1 Bedrock and surficial geology

The study area covers two distinct geological districts (Fig. 1). The southern and western portion is underlain by the flat-lying Paleozoic sedimentary successions of the Western Interior Platform while the northern portion of the study area, including the Yellowknife region, rests on Canadian Shield consisting of the Archean to Neo-Proterozoic rocks of the Slave Geological Province.

The bedrock of the Western Interior Platform is composed of Cambro-Ordovician to Devonian quartz-rich and carbonate sandstone, mudstone, dolomite, and limestone (Rhodes et al., 1984). Bedrock of the WIP is overlain by veneers of fine-grained glaciolacustrine sediments associated with Glacial Lake McConnell that formed following deglaciation of the region between 10,000 and 9,600 ^{14}C yr BP (Smith, 1994; Dyke, 2004). Till deposits range from <1 to 3 m thick to >25 m thick, with thickness increasing locally where karst collapse has created depressions in the bedrock surface. Historic drill hole data show that till can be up to 100 m thick in places (Lemmen, 1990). Till in the area has a silt to fine sand matrix with very little clay (Lemmen, 1998). Till, moraine, and glaciofluvial deposits are extensively reworked into beach deposits composed of bedded sand and gravel (Lemmen, 1998; Gebert, 2008). In other places, fills were washed by wave action that produced a discontinuous coarse lag. Wind action following drainage of the glacial lake formed locally concentrated fine-grained glaciolacustrine sediments into eolian dunes and ridges. Recent deposits in this region include alluvial sediments and organic accumulations in bog and fen settings (Gebert, 2008).

The main bedrock elements of the Slave Geological Province are founded on the granodioritic to tonalitic and related granitoid gneiss of the Central Slave Basement Complex (Bleeker and Davis, 1999) and are composed of the volcanic and turbiditic sedimentary rocks of the Yellowknife Supergroup (Villeneuve et al., 1997). The supracrustal rocks were intruded by several different generations of magma, including syn-volcanic felsic to mafic dykes and sills, three suites of post-Yellowknife Supergroup granites, and Proterozoic intrusions (predominately diabase dykes) (Kjarsgaard et al., 2002). In the Yellowknife study area, the bedrock is dominated by mafic meta-volcanics of the Yellowknife Supergroup (2.71-2.65 Ga; Villeneuve and Relf, 1998) that include basalt, andesite, and pillowed flows that trend north-south and host the major gold deposits. East of Yellowknife, Archean meta-sedimentary rocks predominate and consist of greywacke, slate, schist, and phyllite. Yellowknife Supergroup meta-volcanics and meta-sedimentary rocks are intruded by younger granitoid rocks. West of Yellowknife, granitoid intrusions, consisting of granite, granodiorite, and tonalite, compose the majority of the bedrock. The region is crosscut by several major fault lines, such as the Kam Lake Fault and the West Bay Fault that run through the

city of Yellowknife, separating the volcanic rocks from younger granitoids (Yamashita and Creaser, 1999; Yamashita et al., 1999; Cousens, 2000; Cousens et al., 2002). The region is transected by a variety of un-metamorphosed Proterozoic diabase dykes and over 150 Cretaceous to Eocene kimberlite pipes (Kjarsgaard and Heaman, 1995; Davis and Kjarsgaard, 1997; Kjarsgaard et al., 2002). Numerous greenstone belts (e.g., Courageous Lake greenstone belt) in the Slave Geological Province have resulted in gold exploration and exploitation throughout the region. For detailed description of each component, the reader is referred to Hoffman and Hall (1993), Kjarsgaard et al. (2002), and Helmstaedt et al. (2021). The surficial geology of the Yellowknife region is dominated by a mosaic of Glacial Lake McConnell sediments and glacial tills that infill the topographic lows of the abundant bedrock outcrops. Till is primarily matrix-supported diamicton (Kerr and Wilson, 2000). Clasts consist of various locally derived lithologies and range in size from small pebbles to large boulders. Till in the Yellowknife area may be composed of up to 60% clasts, but most exposures contain approximately 20% to 40% (Kerr and Wilson, 2000). Till exposures have been generally eroded, and are less than 2 m thick, forming discontinuous cover in topographic lows or on bedrock outcrops. Glaciofluvial sediments are relatively uncommon in the study region, and where present consist of fine sand to cobbles in the form of eskers, kames, and outwash (Kerr and Wilson, 2000). A number of surficial sedimentary deposits may be attributed to Glacial Lake McConnell, which infilled Great Slave Lake, Great Bear Lake, and Athabasca Lake basins during deglaciation between 11,800 and 8,300 cal yr BP (Dyke and Prest, 1987; Smith, 1994; Kerr and Wilson, 2000; Wolfe et al., 2014). Sedimentary deposits of Glacial Lake McConnell consist of poorly to moderately sorted coarse to fine sand, silt, and clay that can be up to 20 m thick in some topographic lows (Kerr and Wilson, 2000). These sediments may overlie till, outwash, or bedrock and finer grained sediments deposited in deep water environments and may be overlain by sand and gravel deposited in regressive fluvial or littoral successions. Accumulations of Holocene-aged peat also occur in the study area and can be 1 m thick or greater in bogs and other low-lying wetland types (Kerr and Wilson, 2000).

Further north in the study region, the Lac de Gras area (NTS map sheets 76C and 76D) was covered by the Laurentide Ice Sheet during the last glaciation (Dyke et al., 2002). A transition from southwesterly to northwesterly ice flow occurred during late glacial time (Dredge et al., 1995; Ward et al., 1997). The timing of deglaciation is constrained by a single terrestrial ^{14}C date from plant material contained within an esker of 8500 yr BP, suggesting the landscape was partially deglaciated at this time (Dredge et al., 1995). Sediment cover in this region is mostly composed of a single unstratified till unit. Dredge et al. (1995) and Ward et al. (1997) describe the till as having silty-sandy to sandy matrix and a clast content varying from 5 to 40%. Till can be divided based on surface morphology as well as thickness from till veneer, till blanket, to hummocky till. Till silt content is likely derived from local bedrock sources (granitoids or Yellowknife Supergroup metasediments; Stubley, 2005). Areas of hummocky till have a different geochemical signature to thinner till for some kimberlite pathfinder elements (e.g., Ba, Cr, Mg, Ni; Wilkinson et al., 2001). Variations are attributed to the different bedrock sources of till and transport distances as well as attrition and mixing. Kimberlite indicator minerals such as pyrope, almandine-spessartine garnet, grossular and andradite garnet, diopside, chromite, ilmenite, and olivine are associated with a specific source at transport distances exceeding 70 km (McClenaghan et al., 2002). Modified shaped gold grains with unidentified sources and unknown transport distances are also present (Kerr and Knight, 2007). Potential sources of indicator minerals and till matrix geochemical anomalies include kimberlites, ultramafic dykes, and known volcanogenic massive sulphide

showings as well as a variety of new base, precious, and rare metal showings such as porphyries, alkaline intrusions, and pegmatite. On a landscape scale, stagnant ice associated with the last glaciation created large areas of hummocky till and moraine ridges in the central Slave Geological Province (Kerr et al., 1997). Massive ground ice or icy sediment within till blankets may be present northeast of Contwoyto Lake, evidenced by stabilized thawslides (Wolfe, 2000). Glaciofluvial sediment in the region is commonly contained within tracts of thin or scoured till and exposed bedrock and consists of fine sand to cobbles in the form of eskers, kames, and proglacial outwash (Wolfe, 2000). The tracts, or "corridors" are oriented towards the west or northwest. The relative influence of subglacial scouring, meltwater erosion, and proglacial stagnant water on the origin of these corridors is still debated. Eskers range from small ridges a few tens of metres long to large complexes up to 32 km long and 20-30 m high. Outwash plains with braided channels and kettle lakes are sometimes associated with eskers (Wolfe, 2000). A number of erosional and depositional shoreline landforms associated with a sequence of proglacial lakes that formed in the region surrounding Contwoyto Lake during the last deglaciation are present. These include perched deltas, raised beaches, terraces and spits, wave-cut beaches and washed boulder till surfaces that occur up to 45 m above present lake level (Kerr et al., 1997). Alluvial sediments consisting of gravel and silt-sized sediment deposited by modern streams and rivers are also present (Wolfe, 2000). Accumulations of peat up to 1 m thick are present in topographic lows and poorly drained areas.

Due to the high mineral potential of bedrock in the central Slave Geological Province a large body of literature exists on bedrock geochemistry, but data for Hg is lacking for granitoids, meta-sedimentary, and meta-volcanic rocks in the region (see Table 3 in Galloway et al., 2015). Mercury is documented in early quartz lenses of the Con system (1-0.1 %; along with Pb), in early quartz veins of the Negus-Rycon system (0.1-0.01%), and in quartz-carbonate stringers that cut early quartz lenses of the Campbell system (0.1-0.01%) (values are semi-quantitative spectrographic analyses by the then Spectrographic Laboratory of the Geological Survey of Canada) (table 45, p. 164 in Boyle, 1961). Global values for Hg in continental crust are 0.05 $\mu g \cdot g^{-1}$ (Rudnick and Gao, 2004 and references therein). Tills in the Yellowknife region can contain As with concentrations up to 1560 $mg \cdot kg^{-1}$ within *in situ* weathered material over mineralized zones, but Hg has generally been reported as less than analytical detection limits (Kerr, 2006). The concentration of Hg in glaciofluvial, glaciolacustrine, and peat deposits in the region are either not published or are poorly known due to a lack of regional studies. Pelletier et al. (2021) assessed Hg in six bogs in the Yellowknife region and report Hg concentrations of 42 ± 15 $\mu g \cdot kg^{-1}$ (n=172, max 96 $\mu g \cdot kg^{-1}$) in pre-industrial peat samples. Mercury then peaks to between ~140-250 $\mu g \cdot kg^{-1}$ in cores corresponding to peat that accumulated between 1950 and 1980 and then returns to pre-industrial concentrations in the uppermost layers of peat.

3. METHODS

3.1 Sampling

One hundred and seventy-seven near-surface sediment samples from 169 lakes were collected during the summer and fall seasons from 2009 to 2014 from either canoes or helicopters. The sediment samples were collected from four main regions: the Western Interior Platform, Yellowknife area, Ingraham Trail, and the Tibbitt to Contwoyto Winter Road (Figures 1, 2, 3, 4;

Table 1). The maximum depth (Z_{max}) of each lake was targeted by sampling near the centre of each lake, but bathymetric data does not exist for most of the studied lakes. For some sites, such as Lake 15 (Great Slave Lake) the maximum depth was not sampled as the site was near shore. Metadata and water quality variables (e.g., dissolved oxygen, temperature, pH) were measured at one metre depth intervals in the water column using a multi-metre probe at the time of collection for most lakes. These results are reported in Galloway et al. (2012) and Macumber et al. (2012). Near-surface sediments were collected using an Ekman grab sampler and were predominantly organic-rich fine-grained material (see Galloway et al., 2012, 2015, 2018 and Macumber et al., 2012, 2018 for additional descriptions of grain size data and organic matter characterization for most of the samples). The top 2 to 5 cm of sediment retrieved in the Ekman grab sampler was sub-sampled for element geochemical analyses and other analyses not reported here. The near-surface sediments (upper 2-5 cm) will undoubtedly represent several decades of sediment accumulation in the low sedimentation sub-arctic lakes sampled. Samples were kept cool in the field and during shipping to Carleton University where they were kept cold at 4 °C prior to geochemical analyses.

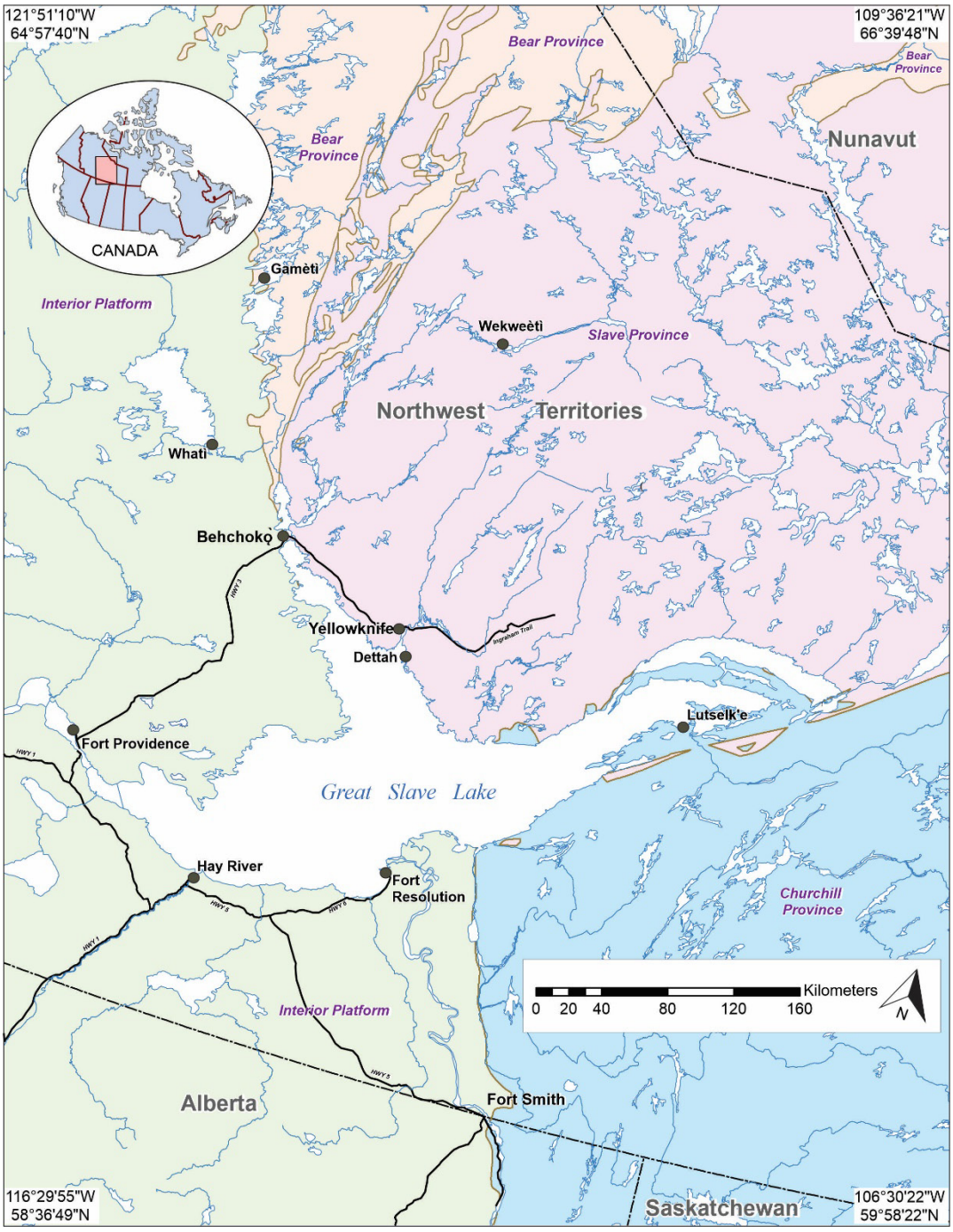

Figure 1: Map of the study region.

Lakes were categorized by their geospatial location (Table 1). Lakes underlain by Western Interior Province bedrock were classified as "Western Interior Province" (WIP) lakes (Fig. 2). Lakes underlain by Slave Geological bedrock components east of Behchokǫ̀ to -114.1574° longitude were classified as "Yellowknife area" lakes (Fig. 3). This area is grouped together because it is the region expected to be impacted by downwind atmospheric deposition from the former Giant Mine (Galloway et al., 2012, 2015, 2018; Palmer et al., 2015; Jasiak et al., 2021). Lakes east of

114.1574° longitude were classified as “east and southeast of Yellowknife along the Ingraham Trail” lakes (Fig. 3). Lakes located along the Tibbitt to Contwoyto Winter Road north of the Ingraham Trail were classified as Tibbitt to Contwoyto Winter Road (TCWR) lakes (Fig. 4).

Figure 2: Map of the study lakes in the Western Interior Platform region. Location of lakes CL2 and HW3-1 studied by Pelletier et al. (2021) shown by blue symbol.

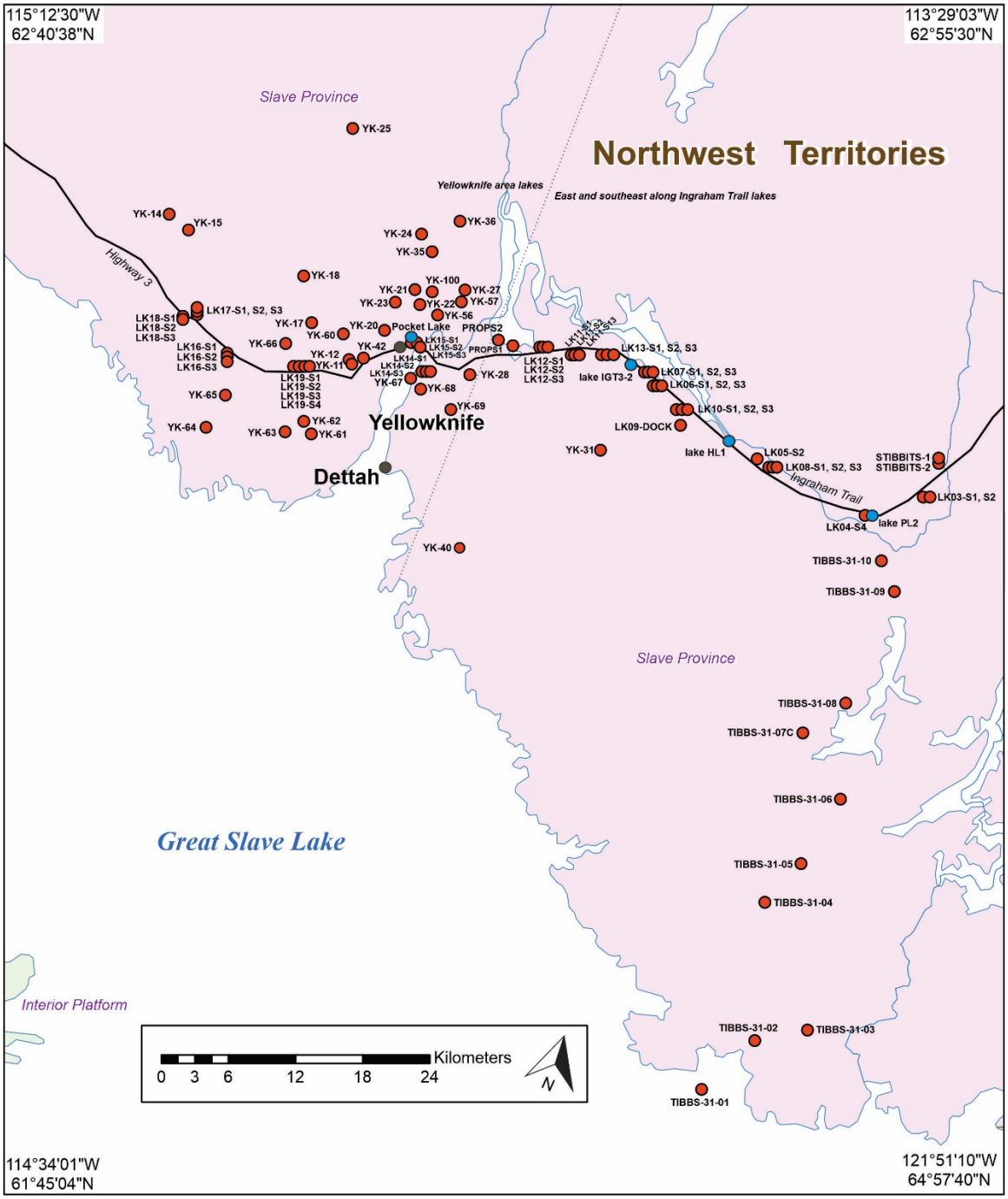

Figure 3: Map of the study lakes in the Yellowknife area and east and southeast along the Ingraham trail area. Dashed line delineates lakes assigned to the "Yellowknife area" and those assigned to the "east and southeast along the Ingraham Trail" region. Location of lakes IGT3-1, HL1, and PL2 studied by Pelletier et al. (2021) and of Pocket Lake (Thienpoint et al., 2016; Patterson et al., 2017; Hutchinson et al., 2019; Hamilton et al., 2021) shown by blue symbol.

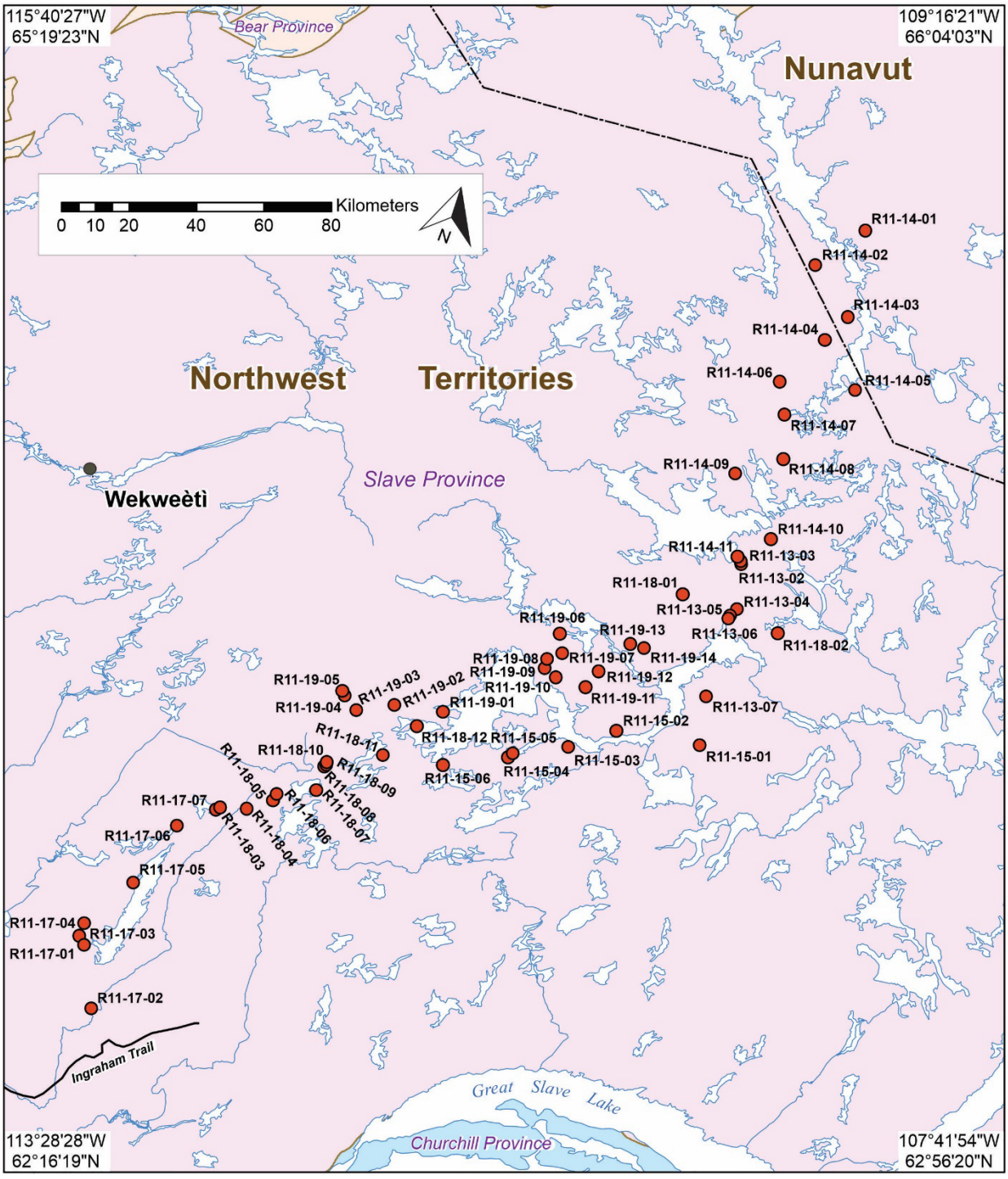

Figure 4: Map of the study lakes along the Tibbitt to Contwoyto Winter Road.

3.2 Mercury analysis

Mercury data derived from ICP-MS for the lakes herein studied are reported in Galloway et al. (2015). In this report, we present total Hg measured using thermal decomposition followed by amalgamation and atomic absorption spectrometry in the near-surface sediments of 169 lakes in the Yellowknife area and surrounding regions. Mercury analysis using thermal decomposition followed by atomic absorption spectrometry generally offers better detection limits than ICP-MS analysis, reduces the likelihood of contamination or Hg loss through volatilization during traditional digestion, is a sensitive method, and is appropriate for small sample sizes (Hall and Pelchat, 1997; Leiva et al., 2013).

Total Hg concentration was determined on freeze-dried sub-samples (average mass 68 mg) by the Geological Survey of Canada in Dartmouth, Nova Scotia, using a Leco AMA-254 Direct Mercury Analyzer. Samples were thermally decomposed at 750°C, followed by collection of the Hg vapour on a gold amalgamator and measurement by atomic absorption spectrophotometry. Replicate samples (n=10) were analyzed to assess analytical precision. Mean Relative Percent Difference (RPD) is 4.6 ± 4.4 SD $\mu g \cdot kg^{-1}$. One sediment certified reference material from the National Research Council of Canada (MESS-3, n=9) was used to assess analytical accuracy. For MESS-3, mean measured Hg concentration is 94.4 ± 1.8 $\mu g \cdot kg^{-1}$ (n=9) versus a certified concentration of 91 ± 9 $\mu g \cdot kg^{-1}$. The standard HISS-1 was also used (n=9), that has mean measured Hg concentration is 5.5 ± 0.4 SD $\mu g \cdot kg^{-1}$ (n=9) versus a provisional concentration of 10 $\mu g \cdot kg^{-1}$ that has been routinely measured as being 5-6 $\mu g \cdot kg^{-1}$ in GSC laboratories. Elemental analyses, organic geochemistry (sequential pyrolysis), and sedimentary grain size for most of the samples reported here are reported in Galloway et al. (2012, 2015, and 2018) and Macumber et al. (2012, 2018). Surface water chemistry of the lakes along the TCWR are reported in Macumber et al. (2012) and for the Yellowknife region in Palmer et al. (2015).

Statistical analyses of total Hg data in lake sediments were conducted using JASP 0.16.4 (JASP, 2022) to determine if total Hg concentration in the near-surface sediment samples varied by region. A Levene's test for equality of variance showed that the data did not meet the assumption of homogeneity of variance (F=5.948, p<0.001) needed for use of the parametric ANOVA test. A non-parametric alternative was thus needed and the Kruskal-Wallis test with Dunn's post-hoc comparisons was used (Dunn, 1961).

RESULTS AND DISCUSSION

Of the 177 samples analyzed, two samples (LK0601, LK0603) had insufficient material for Hg analysis. Three samples (LK19S1, R11-15-002, R11-14-01) had Hg concentrations below detection (5 $\mu g \cdot kg^{-1}$); a value of half the method detection limit was used (2.5 $\mu g \cdot kg^{-1}$) for statistical analyses. Mercury concentrations ranged from 3 to 317 $\mu g \cdot kg^{-1}$ with a median of 68 $\mu g \cdot kg^{-1}$ (n=175) (Table 1).

Table 1: Total Hg concentration measured in near-surface lake sediment samples, replicates, and certified reference material MESS-3 and the internal standard HISS-1.

Sample ID	C-number	Latitude (°N)	Longitude (°W)	Location	Mass (g)	Hg ($\mu g \cdot kg^{-1}$)	Replicate Hg ($\mu g \cdot kg^{-1}$)	MESS-3 ($\mu g \cdot kg^{-1}$)	HISS-1 ($\mu g \cdot kg^{-1}$)
STA11-28-01	C-594972	61.67243	-117.06048	WIP	0.0445	102		95	5
STA11-30-8	C-594988	61.74849	-116.85182	WIP	0.0425	47			
R1-28-005	C-594956	60.90892	-116.82162	WIP	0.0724	36		93	5
STA11-27-01	C-594970	61.83913	-116.67232	WIP	0.1001	37			
R1-29-002	C-594958	60.83825	-116.65584	WIP	0.0537	74			
R-1-28-004	C-492500	60.85864	-116.64240	WIP	0.0750	9	8	97	5
STA11-28-02	C-594973	61.86370	-116.60673	WIP	0.0907	52		98	5
STA11-28-03	C-594974	61.89174	-116.53633	WIP	0.0514	53			
STA11-27-02	C-594971	61.93053	-116.52050	WIP	0.0646	49	47		
STA11-28-04	C-594975	61.91053	-116.51804	WIP	0.0808	32			
STA11-29-03	C-594980	62.49568	-116.50539	WIP	0.0642	32			
STA11-28-05	C-594976	61.96031	-116.48962	WIP	0.0755	45			
R1-28-003	C-492498	60.71001	-116.47049	WIP	0.0766	26			
STA11-28-06	C-594977	61.97038	-116.46828	WIP	0.0686	31	29		
STA11-29-01	C-594978	61.99809	-116.33340	WIP	0.0588	59			
R1-28-002	C-492496	60.45878	-116.32983	WIP	0.0991	9			
STA11-30-6	C-594986	62.00537	-116.29070	WIP	0.0803	33			
STA11-30-07	C-594987	61.90920	-116.28411	WIP	0.0789	31			
STA11-29-2	C-594979	62.15538	-116.26456	WIP	0.0766	21			
STA11-30-05	C-594985	62.09084	-116.25677	WIP	0.0368	87			
STA11-30-04	C-594984	62.10913	-116.20831	WIP	0.0549	77			
STA11-30-2	C-594982	62.25830	-116.19569	WIP	0.0831	20	21	96	5
STA11-30-03	C-594983	62.21984	-116.13657	WIP	0.1021	7		95	
STA11-30-01	C-594981	62.32372	-116.03162	WIP	0.0605	25			
R2-28-001	C-594960	60.69432	-115.90900	WIP	0.0992	31			
R5-27-001	C-594962	60.72066	-114.99526	WIP	0.0385	32	33		
R5-27-002	C-594964	60.71414	-114.96314	WIP	0.0497	25			
R5-27-003	C-594966	60.71875	-114.96314	WIP	0.0431	30			
R5-29-001	C-594968	60.52633	-114.59249	WIP	0.0383	95			
YK14 - 14	C-492411	62.55730	-114.80565	YK area	0.0509	59			
YK14 - 15	C-492412	62.54995	-114.76414	YK area	0.0271	103			
LK18 S2	C-492041	62.48067	-114.72672	YK area	0.1019	75			
LK17 S2	C-492038	62.48600	-114.70723	YK area	0.0941	73	74		
LK17 S1	C-492037	62.48637	-114.70687	YK area	0.0719	105			
LK17-S3	C-492039	62.48573	-114.70332	YK area	0.0709	89		95	5
LK16-S1	C-492034	62.46052	-114.63576	YK area	0.0981	39	40	95	5
LK16 S3	C-492036	62.46443	-114.63518	YK area	0.0370	70			
LK16 S2	C-492035	62.46000	-114.63448	YK area	0.1021	52			

Sample ID	C-number	Latitude (°N)	Longitude (°W)	Location	Mass (g)	Hg ($\mu g \cdot kg^{-1}$)	Replicate Hg ($\mu g \cdot kg^{-1}$)	MESS-3 ($\mu g \cdot kg^{-1}$)	HISS-1 ($\mu g \cdot kg^{-1}$)
YK14 - 64	C-492434	62.39999	-114.62997	YK area	0.0683	127	126		
YK14 - 65	C-492435	62.42961	-114.61933	YK area	0.1006	94			
LK18-S3	C-492042	62.48045	-114.57787	YK area	0.0517	143			
LK18 S1	C-492040	62.48045	-114.57787	YK area	0.0710	120	114		
YK14 - 18	C-492414	62.54205	-114.54423	YK area	0.0244	157			
YK14 - 25	C-492420	62.67065	-114.53847	YK area	0.0525	36			
YK14 - 66	C-492436	62.47304	-114.53817	YK area	0.0243	171			
LK19 S3	C-492045	62.47105	-114.50717	YK area	0.1027	7			
LK19-S4	C-492046	62.46678	-114.50563	YK area	0.1004	6			
LK19 S1	C-492043	62.46678	-114.50563	YK area	0.1044	2.5			
LK19 S2	C-492044	62.47019	-114.50455	YK area	0.1023	22	22		
YK14 - 17	C-492413	62.50749	-114.50319	YK area	0.0277	68			
YK14 - 63	C-492433	62.41479	-114.49336	YK area	0.0791	75	71		
YK14 - 56	C-492428	62.42936	-114.46701	YK area	0.0577	87			
YK14 - 62	C-492432	62.42936	-114.46701	YK area	0.0259	75			
YK14 - 60	C-492430	62.50549	-114.44806	YK area	0.0272	220		92	6
YK14 - 61	C-492431	62.42025	-114.44477	YK area	0.0652	115			
YK14 - 12	C-492410	62.48638	-114.42476	YK area	0.0270	142		95	5
YK14 - 11	C-492409	62.48453	-114.41609	YK area	0.0249	249		90	5
YK14 - 23	C-492418	62.53063	-114.40330	YK area	0.0223	78		90	6
YK14 - 42	C-492427	62.49129	-114.39684	YK area	0.0249	70			
YK14 - 21	C-492416	62.54353	-114.37782	YK area	0.0247	189			
YK14 - 20	C-492415	62.52005	-114.37501	YK area	0.0982	158			
YK14 - 24	C-492419	62.61440	-114.37312	YK area	0.0252	223			
YK14 - 35	C-492424	62.59376	-114.33630	YK area	0.0257	127			
YK14 - 22	C-492417	62.54876	-114.32846	YK area	0.0491	18	18		
LK15 S1 (Great Slave Lake)	C-492031	62.51757	-114.32483	YK area	0.0916	9			
LK15-S2 (Great Slave Lake)	C-492032	62.51465	-114.32465	YK area	0.1007	7			
LK15 S3 (Great Slave Lake)	C-492033	62.51452	-114.32457	YK area	0.1022	6			
YK14 - 100	C-492440	62.56105	-114.31680	YK area	0.0832	23		92	6
YK14 - 36	C-492425	62.62372	-114.30857	YK area	0.0433	178	189		
YK14 - 67	C-492437	62.48871	-114.30478	YK area	0.0792	80			
YK14 - 69	C-492439	62.45355	-114.29527	YK area	0.0547	113			
YK14 - 57	C-492429	62.54524	-114.29250	YK area	0.0638	19	19		
LK14 S2	C-492029	62.49635	-114.28920	YK area	0.0590	44			
LK14-S1	C-492028	62.49728	-114.28815	YK area	0.1002	20			
LK14 S3	C-492030	62.49635	-114.28795	YK area	0.0958	34			

Sample ID	C-number	Latitude (°N)	Longitude (°W)	Location	Mass (g)	Hg ($\mu g \cdot kg^{-1}$)	Replicate Hg ($\mu g \cdot kg^{-1}$)	MESS-3 ($\mu g \cdot kg^{-1}$)	HISS-1 ($\mu g \cdot kg^{-1}$)
YK14 - 68	C-492438	62.48080	-114.28418	YK area	0.0808	82			
YK14 - 27	C-492421	62.57175	-114.25936	YK area	0.0791	38			
YK14 - 28	C-492422	62.50683	-114.20079	YK area	0.0640	56			
PROPS2 (Prosperous Lake Site 2)	C-492048	62.53833	0.00000	E and SE along IT	0.0826	31			
PROPS1 (Prosperous Lake Site 1)	C-492047	62.53939	-114.14745	E and SE along IT	0.0990	16			
YK14 - 40	C-492426	62.36688	-114.13094	E and SE along IT	0.0552	160			
LK12 S2	C-492023	62.53906	-114.12010	E and SE along IT	0.0668	46			
LK12-S1	C-492022	62.62639	-114.11667	E and SE along IT	0.0514	57			
LK13 S3	C-492027	62.55207	-114.02680	E and SE along IT	0.0371	26			
LK13-S1	C-492022	62.55207	-114.02680	E and SE along IT	0.1019	12	14	93	5
LK13-S2 (Pontoon Lake)	C-492026	62.54992	-114.02227	E and SE along IT	0.1034	11			
LK06-S1	C-492006	62.64306	-113.96667	E and SE along IT	INS	INS		99	5
LK06 S2	C-492007	62.54638	-113.96182	E and SE along IT	0.0175	129			
LK06 S3	C-492008	62.62639	-113.95000	E and SE along IT	INS	INS			
YK14 - 31	C-492423	62.47740	-113.94591	E and SE along IT	0.0611	65			
LK07 S2	C-492010	62.54983	-113.94040	E and SE along IT	0.0248	124			
LK07 S3	C-492011	62.54850	-113.93673	E and SE along IT	0.0453	93			
LK-07S1	C-492009	62.54727	-113.93355	E and SE along IT	0.0324	124		94	5
LK11 S3	C-492021	62.54910	-113.91097	E and SE along IT	0.0508	86			
LK11-S1	C-492019	62.54830	-113.91013	E and SE along IT	0.0671	101			
LK11 S2	C-492020	62.54622	-113.90460	E and SE along IT	0.0609	78			
LK09-DOCK	C-492015	62.52159	-113.82844	E and SE along IT	0.1023	40			
LK10 S2	C-492017	62.52472	-113.82657	E and SE along IT	0.0894	25	24		
LK10-S3	C-492018	62.52450	-113.82573	E and SE along IT	0.0852	54			
LK10-S1	C-492016	62.52450	-113.82573	E and SE along IT	0.1029	44			
LK05 S2	C-492005	62.50777	-113.67552	E and SE along IT	0.0514	86			
LK05-S1	C-492004	62.50766	-113.67342	E and SE along IT	0.0530	72			
LK08 S2	C-492013	62.50523	-113.65068	E and SE along IT	0.0451	87			
LK08-S1	C-492012	62.50417	-113.64973	E and SE along IT	0.0547	50			
LK08-S3	C-492014	62.50428	-113.64926	E and SE along IT	0.0806	69			
TIBBS-31-10	C-594998	62.47555	-113.46106	E and SE along IT	0.0325	121			
LK04-S4	C-492003	62.48995	-113.45557	E and SE along IT	0.1030	13	13		
TIBBS-31-07C	C-594995	62.30450	-113.45501	E and SE along IT	0.0585	44			
TIBBS-31-001	C-594989	61.99711	-113.44259	E and SE along IT	0.0461	104			
TIBBS-31-04	C-594992	62.16040	-113.43043	E and SE along IT	0.0465	53		96	5
LK03-S1	C-492001	62.50238	-113.40133	E and SE along IT	0.0388	139			

Sample ID	C-number	Latitude (°N)	Longitude (°W)	Location	Mass (g)	Hg ($\mu g \cdot kg^{-1}$)	Replicate Hg ($\mu g \cdot kg^{-1}$)	MESS-3 ($\mu g \cdot kg^{-1}$)	HISS-1 ($\mu g \cdot kg^{-1}$)
LK03 S2	C-492002	62.50173	-113.39903	E and SE along IT	0.0152	138			
TIBBS-31-08	C-594996	62.33717	-113.39357	E and SE along IT	0.0651	20			
TIBBS-31-05	C-594993	62.19918	-113.38862	E and SE along IT	0.0403	58	57		
TIBBS-31-002	C-594990	62.04831	-113.37816	E and SE along IT	0.1031	59	61		
TIBBS-31-09	C-594997	62.43668	-113.36661	E and SE along IT	0.0422	111			
STIBBITS-1 (Tibbitt Lake Site 1)	C-492049	62.53993	-113.36258	E and SE along IT	0.0247	47			
STIBBITS-2 (Tibbitt Lake Site 2)	C-492050	62.54909	-113.35643	E and SE along IT	0.0354	59			
TIBBS-31-06	C-594994	62.25950	-113.35405	E and SE along IT	0.0545	65			
TIBBS-31-03	C-594991	62.06943	-113.29423	E and SE along IT	0.0581	91			
R11-17-001	C-492464	62.84931	-113.33131	TCWR	0.0271	89	82		
R11-17-04	C-492467	63.01542	-113.30490	TCWR	0.0277	151			
R11-17-03	C-492466	62.95324	-113.45215	TCWR	0.0288	30	33		
R11-17-02	C-492465	62.77065	-113.25791	TCWR	0.0988	72			
R11-17-05	C-492468	63.13537	-113.23034	TCWR	0.0993	96	97		
R11-17-06	C-492469	63.31845	-113.07420	TCWR	0.0506	112		94	5
R11-17-07	C-492470	63.39178	-112.87425	TCWR	0.0564	118			
R11-18-03	C-492473	63.40085	-112.85029	TCWR	0.0529	120			
R11-18-04	C-492474	63.41743	-112.69307	TCWR	0.0588	76			
R11-18-05	C-492475	63.45836	-112.55385	TCWR	0.0558	165			
R11-18-06	C-492476	63.47729	-112.54064	TCWR	0.0999	141			
R11-19-05	C-492487	63.79947	-112.32262	TCWR	0.0539	91			
R11-18-07	C-492477	63.51713	-112.31428	TCWR	0.0584	317			
R11-18-08	C-492478	63.58694	-112.30565	TCWR	0.1009	38	42		
R11-19-04	C-492486	63.78834	-112.29905	TCWR	0.0728	80			
R11-18-10	C-492480	63.60047	-112.29773	TCWR	0.0534	81		94	6
R11-18-09	C-492479	63.59352	-112.29436	TCWR	0.0606	101		95	6
R11-19-03	C-492485	63.75898	-112.20720	TCWR	0.0545	41			
R11-19-02	C-492484	63.79972	-111.98586	TCWR	0.0796	116			
R11-18-11	C-492481	63.65887	-111.97469	TCWR	0.0655	79			
R11-18-12	C-492482	63.76055	-111.82126	TCWR	0.0686	93			
R11-19-01	C-492483	63.81643	-111.68476	TCWR	0.0678	72			
R11-15-006	C-492463	63.67643	-111.60159	TCWR	0.0982	106			
R11-15-005	C-595003	63.74023	-111.28787	TCWR	0.1017	2.5			
R11-15-004	C-492462	63.74194	-111.22387	TCWR	0.0685	76			
R11-19-08	C-492490	64.00433	-111.14232	TCWR	0.0684	50		98	5
R11-19-09	C-595004	63.98293	-111.13927	TCWR	0.0600	104			
R11-19-06	C-492488	64.10607	-111.10594	TCWR	0.0645	89			
R11-19-10	C-492491	63.98798	-111.06110	TCWR	0.0996	53			

Sample ID	C-number	Latitude (°N)	Longitude (°W)	Location	Mass (g)	Hg ($\mu g \cdot kg^{-1}$)	Replicate Hg ($\mu g \cdot kg^{-1}$)	MESS-3 ($\mu g \cdot kg^{-1}$)	HISS-1 ($\mu g \cdot kg^{-1}$)
R11-19-07	C-492489	64.05579	-111.05965	TCWR	0.0736	63	63		
R11-15-003	C-492461	63.81104	-110.87622	TCWR	0.0632	69			
R11-19-11	C-492492	63.98221	-110.86615	TCWR	0.0947	158			
R11-19-12	C-492493	64.03270	-110.80939	TCWR	0.0732	115			
R11-19-13	C-492494	64.12713	-110.66071	TCWR	0.0711	48			
R11-15-02	C-492460	63.88657	-110.61165	TCWR	0.1019	48	46	94	5
R11-19-14	C-492495	64.12511	-110.56963	TCWR	0.1000	36			
R11-18-01	C-492471	64.29394	-110.41670	TCWR	0.0758	80			
R11-14-009	C-492456	64.64986	-110.27483	TCWR	0.0796	42			
R11-14-11	C-492458	64.43018	-110.13640	TCWR	0.1009	5	5		
R11-14-006	C-492453	64.92442	-110.13530	TCWR	0.1000	85			
R11-13-07	C-492447	64.03700	-110.11820	TCWR	0.0901	60			
R11-13-03	C-492443	64.41946	-110.10531	TCWR	0.0788	78			
R11-13-02	C-492442	64.41210	-110.10004	TCWR	0.1010	11			
R11-13-06	C-492446	64.25860	-110.09870	TCWR	0.0848	70			
R11-13-05	C-492445	64.26840	-110.09290	TCWR	0.0956	74			
R11-14-002	C-492449	65.25836	-110.09042	TCWR	0.0996	7			
R11-15-001	C-492459	63.90215	-110.08659	TCWR	0.0863	75			
R11-13-04	C-492444	64.28980	-110.06040	TCWR	0.0814	58			
R11-14-007	C-492454	64.83945	-110.05595	TCWR	0.0987	79			
R11-13-01	C-492441	64.33320	-110.00037	TCWR	0.1017	2.5		92	5
R11-14-008	C-492455	64.72008	-109.99793	TCWR	0.1009	14			
R11-14-010	C-492457	64.49888	-109.95382	TCWR	0.0733	119	121		
R11-14-004	C-492451	65.06421	-109.91413	TCWR	0.1003	17			
R11-14-001	C-492448	65.38336	-109.82280	TCWR	0.0643	60			
R11-14-003	C-492450	65.14045	-109.80222	TCWR	0.0992	47	48	95	6
R11-18-02	C-492472	64.25149	-109.77301	TCWR	0.0765	97			
R11-14-005	C-492452	64.94988	-109.64731	TCWR	0.0624	50			

C-number = GSC Curation number; INS = insufficient material for analyses; WIP = Western Interior Platform; YK area = Yellowknife area; E and SE along IT = east and southeast of Yellowknife along Ingraham Trail; TCWR = Tibbitt to Contwoyto Winter Road (see Figs. 2, 3, and 4 for map of study lakes for each region).

The total Hg concentrations include some values that are above the Canadian Council Ministers of Environment Interim Sediment Quality Guideline for Freshwater of 170 $\mu g \cdot kg^{-1}$ (CCME, 1999). This guideline was exceeded in 18 (10%) of samples. The only areas where sedimentary Hg concentration in near-surface sediments did not exceed the ISQG level for Hg were those in the Western Interior Province and east and southeast of Yellowknife along the Ingraham Trail (Tables 1, 2; Fig. 5). The concentration of Hg in all samples is below the Probable Effect Level of 486 $\mu g \cdot kg^{-1}$ (CCME, 1999).

Table 2: Total Hg concentration (median min, max, µg·kg^{-1}) in near-surface sediments of lakes sampled in different geospatial regions. See Figs. 2, 3, and 4 for location of lakes in each region.

Region	Western Interior Platform	Yellowknife area	East and southeast of Yellowknife along the Ingraham Trail	Tibbitt to Contwoyto Winter Road
Median (min-max)	32 (7-102)	75 (3-249)	62 (11-160)	76 (3-317)
n	29	49	40	57

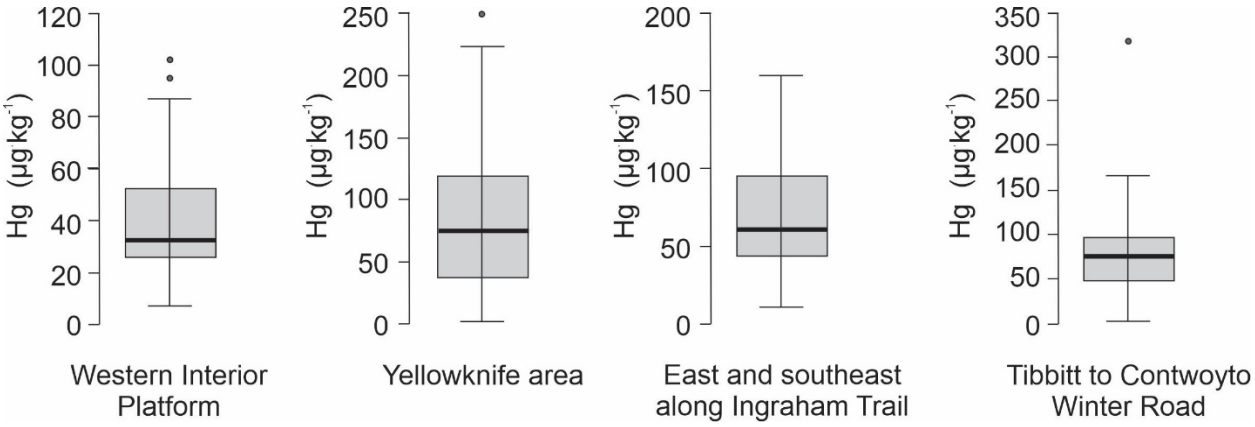

Figure 5: Box-Whisker plots showing minimum value, second quartile, median, third quartile, and maximum value of total Hg concentration in near-surface lake sediments by region (Table 1; Figs. 2, 3, 4). Note differences in scale.

A Kruskal-Wallis test (H=15.689, p=0.001, df=3) shows that the total Hg concentration varies significantly by geospatial location. The pairwise comparison using Dunn's test indicates that sedimentary Hg concentration was significantly lower in sediments of lakes from located in the Western Interior Platform region compared to the other geospatial categories (Table 3). No other differences were statistically significant at the p<0.05 level.

Table 3: Dunn's post hoc comparison of total Hg concentration in sediments of lakes categorized by location. *P*-values <0.05 are in bold italics. P_{bonf} = Bonferroni adjustment; P_{holm} = Holm's Bonferroni correction.

Comparison	z	W_i	W_j	*p*	p_{bonf}	p_{holm}
YK area vs. E and SE along IT	0.616	96.541	89.888	0.538	1	1
YK area vs. TCWR	0.017	96.541	96.377	0.987	1	1
YK area vs. WIP	3.542	96.541	54.5	***<0.001***	***0.002***	***0.002***
E and SE along IT vs. TCWR	-0.621	89.888	96.377	0.535	1	1
E and SE along IT vs. WIP	2.864	89.888	54.5	***0.004***	***0.025***	***0.017***
TCWR vs. WIP	3.624	96.377	54.5	***<0.001***	***0.002***	***0.002***

WIP = Western Interior Platform; YK area = Yellowknife area; E and SE along IT = east and southeast of Yellowknife along Ingraham Trail; TCWR = Tibbitt to Contwoyto Winter Road

The median total Hg concentration in near-surface sediments in lakes from the Yellowknife area, east and southeast of Yellowknife along the Ingraham Trail, and along the Tibbitt to Contwoyto

Winter road are significantly higher than in sediments of lakes in the Western Interior Platform (Tables 2, 3; Fig. 5). This result suggests that at least some of the accumulated Hg in lakes underlain by Slave Geological Province rocks is associated with the bedrock geology and derived surficial materials. Houben et al. (2016) suggested a potential source of Hg to surface waters in their study of 25 lakes within a 25 km radius of the historic Giant Mine related to the Yellowknife Bay Formation that may have been a source of both Hg and sulfate, and that the sulfate promoted the methylation of the Hg (from geogenic and/or anthropogenic sources) in surface waters. However, Pelletier et al. (2021) report comparable sedimentary Hg concentration in sediments of two lakes from the Taiga Plains and three from the Taiga Shield. Pelletier et al. (2021) report total Hg concentration in lake sediments deposited in pre-industrial times in five lakes in the Taiga Plains and Taiga Shield ecoregions as ranging between 28 ± 3 $\mu g \cdot kg^{-1}$ and 47 ± 5 $\mu g \cdot kg^{-1}$. Three of the lakes are located on Taiga Shield (Lake PL2, HL1, IGT3-2) (Fig. 3). In the sediment of those lakes, Hg deposited in pre-industrial times (pre-1940) ranged from 32 to 35 $\mu g \cdot kg^{-1}$ (lake PL2), from 23 to 54 $\mu g \cdot kg^{-1}$ (lake HL1), and from 43 to 75 $\mu g \cdot kg^{-1}$ (lake IGT3-2). In sediments deposited after 1940, Hg ranged from 35 to 48 $\mu g \cdot kg^{-1}$ (lake PL2), 33 to 72 $\mu g \cdot kg^{-1}$ (lake HL1), and 62 to 133 $\mu g \cdot kg^{-1}$ (lake IGT3-2) (Pelletier et al., 2021). In the two lakes located in the Taiga Plains (Fig. 2), sedimentary Hg concentrations ranged from 32-85 $\mu g \cdot kg^{-1}$ in pre-1940 sediment and from 30-56 $\mu g \cdot kg^{-1}$ in post-1940 sediment in lake HW3-1 and from 34-56 $\mu g \cdot kg^{-1}$ in pre-1940 sediment and from 22-66 $\mu g \cdot kg^{-1}$ in post-1940 sediment in lake CL2.

The lake sediment Hg concentrations reported by Pelletier et al. (2021) are comparable to the median Hg concentration in near-surface lake sediments of the Yellowknife area (75 $\mu g \cdot kg^{-1}$), east and southeast of Yellowknife along the Ingraham Trail area (62 $\mu g \cdot kg^{-1}$), along the Tibbitt to Contwoyto Winter Road (76 $\mu g \cdot kg^{-1}$), and of the Western Interior Platform area (32 $\mu g \cdot kg^{-1}$), but the range in sedimentary Hg values reported here are greater (Table 2) (Western Interior Platform 7-102 $\mu g \cdot kg^{-1}$; Yellowknife area 3-249 $\mu g \cdot kg^{-1}$, east and southeast along Ingraham Trail 11-160 $\mu g \cdot kg^{-1}$; Tibbitt to Contwoyto Winter Road 3-317 $\mu g \cdot kg^{-1}$), reflecting the larger sample size and variations in organic matter, as well as possibly grain size, mineral input, catchment and lake area, and climate.

CONCLUSIONS

Total Hg concentration ranged from 3 to 317 $\mu g \cdot kg^{-1}$ in 175 near-surface sediments collected from 169 lakes in the central Northwest Territories. Total sedimentary Hg concentration is significantly lower (median 32 $ug \cdot kg^{-1}$, range 7-102 $ug \cdot kg^{-1}$) in lakes underlain by Western Interior Platform bedrock than in lakes underlain by Slave Geological Province bedrock. Future work is needed to focus on the mobility and fate of Hg in high northern latitude environments.

REFERENCES

Bleeker, W., Davis, W.J. (1999). The 1991-1006 NATMAP Slave Province Project: Introduction. Canadian Journal of Earth Science, 36, 1033-1042.

Boyle, R.W. (1961). Geology, geochemistry, and origin of the gold deposits of the Yellowknife District, Northwest Territories. Geological Survey of Canada, Memoir 310, 193 pp. + 12 map sheets.

Canadian Council of Ministers of the Environment (CCME). (1999). Canadian Sediment Quality Guidelines for the Protection of Aquatic Life, Mercury. In: Canadian environmental quality guidelines, 1999, Canadian Council of Ministers of the Environment, Winnipeg, 5 pp.

Cheney, C., Eccles, K.M., Kimpe, L.E., Thienpoint, J.R., Korosi, J.B., Blais, J.M. (2020). Determining the effects of past gold mining using a sediment palaeotoxicity model. Science of the Total Environment, 718, 137308.

Cheung, J. S.-J., Hu, X. F., Parajuli, R. P., Rosol, R., Torng, A., Mohapatra, A., Lye, E., & Chan, H. M. (2020). Health risk assessment of arsenic exposure among the residents in Ndilǫ, Dettah, and Yellowknife, Northwest Territories, Canada. International Journal of Hygiene and Environmental Health, 230, 113623.

Cott, P.A., Zajdlik, B.A., Palmer, M.J., McPherson, M.D. (2016). Arsenic and mercury in lake whitefish and burbot near the abandoned Giant Mine on Great Slave Lake. Journal of Great Lakes Research, 42, 223-232.

Cousens, B.L. (2000). Geochemistry of the Archean Kam Group, Yellowknife greenstone belt, Slave Province, Canada. The Journal of Geology, 108, 181-197.

Cousens, B.L., Facey, K., Falck, H. (2002). Geochemistry of the late Archean Banting Group, Yellowknife greenstone belt, Slave Province, Canada: simultaneous melting of the upper mantle and juvenile mafic crust. Canadian Journal of Earth Sciences, 39, 1635-1656.

Davis, W.J., Kjarsgaard, B.A. (1997). A Rb-Sr isochron age for kimberlite from the recently discovered Lac de Gras field, Slave Province, Northwest Territories, Canada. Journal of Geology, 105, 503-509.

Dredge, L.A., Ward, B.C., Kerr, D.E. (1995). Surficial geology, Aylmer Lake, District of Mackenzie, Northwest Territories. Geological Survey of Canada, A Series Map 1867A, 2 sheets.

Dun, O.J. (1961). Multiple comparisons among means. Journal of the Acoustical Society of America (JASA), 56, 54-64.

Dyke, A.S. (2004). An outline of North American deglaciation with emphasis on central and northern Canada, *in,* Gibbard, P.L., Ehlers, J. (eds.); Quaternary glaciations – extent and chronology, Part II. North America, 373-424.

Dyke, A.S., Prest, V.K. (1987). Paleogeography of northern North America 11 000 – 8 400 years ago; Geological Survey of Canada, A Series Map 1703A, Sheet 2 of 3, scale 1:12 500 000.

Dyke, A., Andrews, J., Clark, P., England, J., Miller, G., Shaw, J., Veillette, J. (2002). The Laurentide and Innuitian ice sheets during the last glacial maximum. Quaternary Science Reviews, 21, 9-31.

Ecosystem Classification Group. (2007) (rev. 2009). Ecological Regions of the Northwest Territories. Department of Environment and Natural Resources, Government of the Northwest Territories, Yellowknife, NT, Canada.

Galloway, J.M., Sanei, H., Patterson, R.T., Mosstajiri, T., Hadlari, T., Falck, H. (2012). Physical and chemical characterization of Yellowknife area lake sediments, Northwest Territories. Geological Survey of Canada Open File, 7307, 47 pp.

Galloway, J.M., Palmer, M., Jamieson, H.E., Patterson, R.T., Nasser, N.A., Falck, H., Macumber, A.L., Goldsmith, S.A., Sanei, H., Normandeau, P., Hadlari, T., Roe, H.M., Neville, L.A., Lemay, D. (2015). Geochemistry of lakes across ecozones in the Northwest Territories and implications for the distribution of arsenic in the Yellowknife region. Part 1: Sediments; Geological Survey of Canada, Open File 7908, 50 pp. + appendix, 1 .zip file

Galloway, J. M., Swindles, G. T., Jamieson, H. E., Palmer, M., Parsons, M. B., Sanei, H., Macumber, A. L., Timothy Patterson, R., & Falck, H. (2018). Organic matter control on the distribution of arsenic in lake sediments impacted by ~65years of gold ore processing in subarctic Canada. Science of The Total Environment, 622, 1668–1679.

Gebert, J.S. (2008). Ka'a'gee Tu Area of Interest, Phase 1 Non-renewable Resource Assessment – Minerals, Northwest Territories, Parts of NTS 85C, 85D, 85 E and 85 F. Northwest Territories Geoscience Office, NWT Open File 2008-06, 26 pp.

Haitzer, M., Aiken, G. R., Ryan, J. N. (2002). Binding of mercury(II) to dissolved organic matter: the role of the mercury-to-DOM ratio. Environmental Science and Technology, 36, 3564-3570.

Hall, G.E.M., Pelchat, P. (1997) Evaluation of a direct solid sampling atomic absorption spectrometer for the trace determination of mercury in geological samples. Analyst, 122, 921-924.

Hamilton, P., Hutchinson, S., Patterson, R.T., Galloway, J.M., Nasser, N., Spence, C., Palmer, M., Falck, H. (2021). Late Holocene diatom community response to climate driven geochemical changes in a small, subarctic lake, Northwest Territories, Canada. The Holocene, 31, 1124-1137.

Hoffman, P., Hall, L. (1993). Geology, Slave Craton and environs, District of Mackenzie, Northwest Territories. Geological Survey of Canada, Open File 2559, 1 sheet, 1 CD ROM.

Houben, A. J., D'Onofrio, R., Kokelj, S. V, & Blais, J. M. (2016). Factors Affecting Elevated Arsenic and Methyl Mercury Concentrations in Small Shield Lakes Surrounding Gold Mines near the Yellowknife, NT, (Canada) Region. PLOS ONE, 11, e0150960.

Hutchinson, S.J., Hamilton, P.B., Patterson, R.T., Galloway, J.M., Nasser, N.A., Spence, C., Falck, H. (2018). Diatom ecological response to deposition of the 833-850 CE White River Ash (east lobe) ashfall in a small subarctic Canadian lake. PeerJ, 7, e6269.

Indian and Northern Affairs Canada (INAC) (now Crown-Indigenous Relations and Northern Affaris Canada). (2007). Giant Mine remediation plan. Mackenzie Valley Land and Water Board, Yellowknife, Northwest Territories, Canada.

Jasiak, I., Wiklund, J. A., Leclerc, E., Telford, J. V, Couture, R. M., Venkiteswaran, J. J., Hall, R. I., & Wolfe, B. B. (2021). Evaluating spatiotemporal patterns of arsenic, antimony, and lead deposition from legacy gold mine emissions using lake sediment records. Applied Geochemistry, 134, 105053.

Jamieson, H.E., 2014. The legacy of arsenic contamination from mining and processing refractory gold ore at Giant Mine, Yellowknife, Northwest Territories, Canada. Reviews in Mineralogy and Geochemistry, 79, 533–551.

JASP Team (2022). JASP (Version 0.16.3)[Computer software].

Kainz, M., Lucotte, M. (2006). Mercury Concentrations in Lake Sediments – Revisiting the Predictive Power of Catchment Morphometry and Organic Matter Composition. Water Air and Soil Pollution, 170, 173–189.

Kerr, D.E. (1997).Surifical geology, north half of Contwoyto Lake map area (NTS 76E), N.W.T. Geological Survey of Canada, Current Research 1997-C, 51-59.

Kerr, D.E. (2006). Chapter 20, Quaternary Geology and Exploration Geochemistry, *in,* Anglin, C.D., Falck, H., Wright, D.F., Ambrose, E.J. (eds.); GAC Special Publication No.3, Gold in the Yellowknife Greenstone Belt, Northwest Territories: Results of the Extech III Multidisciplinary Research Project, 301-324.

Kerr, D.E., Wilson, P. (2000). Preliminary surficial geology studies and mineral exploration considerations in the Yellowknife area, Northwest Territories. Geological Survey of Canada, Current Research 2000-C3, 8 pp.

Kerr, D.E., Knight, R.D. (2007). Gold grains in till, Slave Province, Northwest Territories and Nunavut. Geological Survey of Canada, Open File 5463, 5 pp.

Kjarsgaard, B.A., Wyllie, R.J.S. (1994). Geology of the Paul Lake area, Lac de Gras – Lac du Sauvage region of the central Slave Province, District of Mackenzie, Northwest Territories. Geological Survey of Canada, Current Research 1994-C, 23-32.

Kjarsgaard, B.A., Heaman, L.M. (1995). Distinct periods of Phanerozoic kimberlites in North America, and implications for the Slave Geological Province, *in,* E.I. Igboji (ed.); Exploration Overview 1995, Northwest Territories. Department of Indian and Northern Affairs, Yellowknife, Northwest Territories, 22-23.

Kjarsgaard, B.A., Wilkinson, L., Armstrong, J. (2002). Geology, Lac de Gras kimberlite field, central Slave Province, Northwest Territories – Nunavut. Geological Survey of Canada, Open File 3238, 1 sheet, 1 CD-ROM.

Lemmen, D.S. (1998). Surifical geology, Buffalo Lake, District of Mackenzie, Northwest Territories. Geological Survey of Canada, A Series Map 1906A, scale 1:250,000, 1 sheet.

Lemmen, D.S. (1990). Surficial materials associated with glacial Lake McConnell, southern District of Mackenzie. Current Research, Part D, Geological Survey of Canada, Paper 90-1D, 79-83.

Leiva G., M.A., Morales, S., Segura, R. (2013) Comparative measurements and their compliance with standards of total mercury analysis in soil by cold vapour and thermal decomposition, amalgamation and atomic absorption spectrometry. Water Air and Soil Pollution, 224, 1390.

Mackenzie Valley Review Board. (2013). Report of Environmental Assessment and reasons for Decision. Giant Mine Remediation Project, Yellowknife, Canada.

Macumber, A.L., Neville, L.A., Galloway, J.M., Patterson, R.T., Falck, H., Swindles, G.T., Crann, C., Clark, I., Gammon, P., Madsen, E. 2012. Paleoclimatological assessment of the Northwest Territories and Implications for the long-term viability of the Tibbitt to Contwoyto Winter Road, Part II: March 2010 field season results. NWT Open Report, 82 pp.

Macumber, A.L., Patterson, R.T., Galloway, J.M., Falck, H., Swindles, G.T. (2018). Reconstruction of Holocene hydroclimatic variability in subarctic treeline lakes using lake sediment grain-size end-members. The Holocene, 28, 845-857.

McClenaghan, M.B., Ward, B.C., Kjarsgaard, I.M., Kjarsgaard, B.A., Kerr, D.E., Dredge, L.A. (2002). Indicator mineral and till geochemical dispersal patterns associated with the Ranch Lake kimberlite, Lac de Gras region, NWT, Canada. Geochemistry: Exploration, Environment, Analysis, 2, 299-319.

Nasser, N.A., Patterson, R.T., Roe, H.M., Galloway, J.M., Falck, H., Palmer, M.J., Spence, C., Sanei, H., Macumber, A.L., Neville, L.A. (2016). Lacustrine Arcellinina (testate amoebae) as bioindicators of arsenic contamination. Microbial Ecology, 72, 130-149.

Outridge, P.M., Sanei, H., Stern, G., Hamilton, P., Goodarzi, F. (2007). Evidence for Control of Mercury Accumulation Rates in Canadian High Arctic Lake Sediments by Variations of Aquatic Primary Productivity. Environmental Science and Technology, 41, 5259–5265.

Outridge, P.M., Stern, G.A., Hamilton, P.B., Sanei, H. (2019). Algal scavenging of mercury in preindustrial Arctic lakes. Limnology and Oceanographthy, 64, 1558-1571.

Palmer, M., Galloway, J.M., Jamieson, H.E., Patterson, R.T., Falck, H., Kokelj, S.V. (2015). The concentration of arsenic in lake waters of the Yellowknife area 15 years after the end of gold ore processing. Northwest Territories Geological Survey, Open File 2015-16, 29 p.

Palmer, M. J., Chételat, J., Richardson, M., Jamieson, H. E., Galloway, J.M. (2019). Seasonal variation of arsenic and antimony in surface waters of small subarctic lakes impacted by legacy

mining pollution near Yellowknife, NT, Canada. Science of the Total Environment, 684, 326-339.

Patterson, R.T., Crann, C.A., Cutts, J.A., Mustaphi, C.J.C., Nasser, N.A., Macumber, A.L., Galloway, J.M., Swindles, G.T., Falck, H. (2017). New occurrences of the White River Ash (east lobe) in sub-arctic Canada and utility for estimating freshwater reservoir effect in lake sediment archives. Palaeogeograpy, Palaeoclimatology, Palaeoecology, 477, 1-9.

Pelletier, N., Chételat, J., Palmer, M.J., Vermaire, J.C. (2021). Bog and lake sediment archives reveal a lagged response of subarctic lakes to diminishing atmospheric Hg and Pb deposition. Science of the Total Environment, 775, 145521.

Persaud, A.A., Cheney, C.L., Sivarajah, B., Blais, J.M., Smol, J.P., Korosi, J.B. (2021). Regional changes in Cladocera (Branchiopoda, Crustacea) assemblages in subarctic (Yellowknife, Northwest Territories, Canada) lakes impacted by historic gold mining activitys. Hydrobiologia 848, 1367-1389.

Rhodes, D., Lantos, E.A., Webb, R.J., Owens, D.C. (1984). Pine Point orebodies and their relationships to the stratigraphy, structure, dolomitization and karstification of the Middle Devonian Barrier Complex. Economic Geology, 79, 991-1055.

Sanei, H., Outridge, P.M., Stern, G.A., Macdonald, R.W. (2014). Classification of mercury-labile organic matter relationships in lake sediments. Chemical Geology, 373, 87-92.

Schuh, C. E., Jamieson, H. E., Palmer, M. J., & Martin, A. J. (2018). Solid-phase speciation and post-depositional mobility of arsenic in lake sediments impacted by ore roasting at legacy gold mines in the Yellowknife area, Northwest Territories, Canada. Applied Geochemistry, 91, 208-220.

Sivarajah, B., Korosi, J.B., Thienpoint, J.R., Kimpe, L.E., Blais, J.M., Smol, J.P., 2022. Algal responses to metal(loid) pollution, urbanization, and climatic changes in subarctic lakes around Yellowknife, Canada. Arctic Science, 8, 1340-1355.

Smith, D.G. (1994). Glacial Lake McConnell: Paleogeography, age, duration, and associated river deltas, Mackenzie River Basin, Western Canada. Quaternary Science Reviews, 13, 829-843.

Stubley, M.P. (2005). Slave Craton: Interpretative bedrock compilation. Northwest Territories Geoscience Office, NWT-NU Open File 2005-01.

Thienpont, J. R., Korosi, J. B., Hargan, K. E., Williams, T., Eickmeyer, D. C., Kimpe, L. E., Palmer, M. J., Smol, J. P., & Blais, J. M. (2016). Multi-trophic level response to extreme metal contamination from gold mining in a subarctic lake. Proceedings of the Royal Society B: Biological Sciences, 283, 20161125.

Van Den Berghe, M. D., Jamieson, H. E., & Palmer, M. J. (2018). Arsenic mobility and characterization in lakes impacted by gold ore roasting, Yellowknife, NWT, Canada. Environmental Pollution, 234, 630–641.

Villeneuve, M.E., Henderson, J.R., Hrabi, R.G.B., Jackson, V.A., Relf, C. (1997). 2.70 – 2.58 Ga plutonism and volcanism in the Slave Province, District of Mackenzie, Northwest Territories. Radiogenic Age and Isotopic Studies: Report 10. Geological Survey of Canada, Current Research 1997-F, 37-60.

Villeneuve, M.F., Relf, C. (1998). Tectonic setting of 2.6 Ga carbonatites in the Slave Province, NW Canada. Journal of Petrology, 38, 1975-1986.

Ward, B.C., Dredge, L.A., Kerr, D.E. 1997. Surficial geology, Lac de Gras, District of Mackenzie, Northwest Territories. Series A Map 1870A, 1 sheet.

Wilkinson, L., Harris, J., Kjarsgaard, B.A., McClenaghan, M.B., Kerr, D.E. 2001. Influence of till thickness and texture on till geochemistry in the Lac de Gras area, Northwest Territories, with applications for regional kimberlite exploration. Geological Survey of Canada, Current Research 2001-C9, 10 p.

Wiken, E.B. 1986. Terrestrial ecozones of Canada, Ecological Land Classification Series No. 19. Lands Directorate, Environment Canada, Hull, Quebec, 26 p. + map.

Wolfe, S.A. (2000). Permafrost research and monitoring stations in west Kitikmeot, Slave geological province, Nunavut. Geological Survey of Canada, Open File 3848, 82 pp.

Wolfe, S.A., Stevens, C.W., Gaanderse, A.J., Oldenborger, G.A. (2014). Lithalsa distribution, morphology and landscape associations in the Great Slave Lowland, Northwest Territories, Canada. Geomorphology, 204, 302-313.

Yamashita, K., Creaser, R.A. (1999). Geochemical and Nd isotopic constraints for the origin of Late Archean turbidites from the Yellowknife area, Northwest Territories, Canada. Geochimica et Cosmochimica Acta, 63, 2579-2598.

Yamashita, K., Creaser, R.A., Stemler, J.U., Zimaro, T.W. (1999). Geochemical and Nd-Pb isotopic systematics of late Archean granitoids, southwestern Slave Province, Canada: constraints for granitoid origin and crustal isotopic structure. Canadian Journal of Earth Sciences, 36, 1131-1147.